

Fabrication of Poly(triazine dithiol) Functional Nanofilm by Galvanostatic Polymerization on Aluminum

Yabin Wang, Shaoju Bian, Xin Liu, Fang Wang* and Qingfen Meng*

¹ Qinghai Institute of Salt Lakes, Chinese Academy of Sciences, Xinning Road No. 18, Xining, Qinghai 810008, PR China

² Northwest Agriculture & Forest University, College of Science, Shaanxi, Yangling 712100, PR China

*E-mail: qfmeng@isl.ac.cn; wangfang4070@nwsuaf.edu.cn

Received: 29 May 2013 / Accepted: 25 June 2013 / Published: 1 August 2013

The functional polymeric nanofilm of 6-(N-allyl-1, 1, 2, 2-tetrahydroperfluorododecyl) amino-1, 3, 5-triazine-2, 4-dithiol monosodium (ATP) was prepared on aluminum surface by galvanostatic polymerization technique. The chemical structure of nanofilm was characterized by Fourier transform infrared spectroscopy (FT-IR) and X-ray photoelectron spectroscopy (XPS). Adsorption peaks in FT-IR and C1s, N1s, S2p and F1s peaks in the XPS spectra indicate that the polymeric nanofilm is successfully fabricated in NaNO₂ electrolyte solution. The influencing factors were investigated by potential and eletropolymerization time curves (*E-t*), XPS spectra, film weight, film thickness and AFM. All the results show that the optimal electrochemical polymerization current, temperature and time are 0.4mA/cm², 15°C and 8min respectively. Uniform and compact polymeric nanofilm of ATP could be obtained under these conditions. It is expected that this technique will be applied in preparation of lubricating, anti-tribological and hydrophobic surface on aluminum with functional triazinedithiols.

Keywords: triazinedithiol monosodium, functional polymeric nanofilms, galvanostatic polymerization, aluminum

1. INTRODUCTION

Since the publication of Mori Kunio's researches on the anticorrosion properties of triazinedithiols (TDTs) on copper surface [1], adsorption and polymerization of TDTs on metal surfaces have been receiving increasing attention in the past few years [2-5]. Research showed that polymeric nanofilms prepared by different TDTs had excellent properties, such as adhesion [6], dielectric property [7], and anticorrosion [8]. 6-(N-allyl-1, 1, 2, 2-tetrahydroperfluorodecyl) amino-1,

3, 5-triazine-2,4-dithiol monosodium (AF17N) is one derivative of the triazinedithiol compounds. The polymeric nanofilm of AF17N (PAF17N) has shown lubrication property [7], anti-tribology property [9], and hydrophobicity [5] owing to the existence of fluorine atoms with the number of seventeen. Therefore, techniques of preparing functional PAF17N have attracted lots of studies. Electropolymerization technique was mainly used to fabricate PAF17N, including cyclic voltammetry [10], one-step potentiostatic [11] and two-step potentiostatic [12] methods. The three electrochemical methods to fabricate PAF17N had been studied systematically.

In order to enhance the functionality of triazinedithiol compound with fluorine atoms, we have successfully synthesized 6-(N-allyl-1, 1, 2, 2-tetrahydroperfluorododecyl) amino-1, 3, 5-triazine-2,4-dithiol monosodium (ATP, figure 1), which possesses more fluorine atoms than AF17N. In this paper, on the one hand, we will focus on the research of preparing PATP nanofilm by galvanostatic technique. On the other hand, the key parameters of galvanostatic technique and influencing factors will also be investigated.

2. EXPERIMENTAL SECTION

2.1. Materials

Test specimens ($50 \times 30 \times 0.1$ mm) of pure aluminum (purity no less than 99.9995%) were prepared by cutting a large surface into pieces. All test surfaces were degreased by ultrasonic washing in acetone for 15min, and dried in nitrogen. ATP was prepared by reaction between 6-(N-allyl-1, 1, 2, 2-tetrahydroperfluorododecyl) amine-1, 3, 5-triazine-2, 4-dichloride and NaSH, according to the method described in previous paper [13]. All of the chemicals were employed as analytical reagent (AR) without further purification. Distilled water was used as solvent, and NaNO₂, Na₂SO₄, NaBO₂, Na₃PO₄, Na₂CO₃ and NaOH were applied as supporting electrolytes. The concentrations of ATP and supporting electrolytes were kept constant at 5 mM and 0.1 M, respectively [14].

2.2. Preparation of PATP by galvanostatic method

The electrochemical polymerization of ATP was performed by using electrochemical measurement apparatus (Hokuto Denkou Co.Ltd., HD-3000). The electrolytic cell was equipped with working electrode (aluminum surfaces), Pt counter electrode, and reference electrode (saturated calomel electrode, SCE), then was filled with electrolytic solution containing ATP. The currents of galvanostatic polymerization ranged from 0.1 to 0.5mA/cm². Polymerization temperature at 5°C, 15°C, 25°C and 35°C were investigated. Polymerization time was also studied. The whole process was conducted without any stirring.

2.3. Characterization

FT-IR spectra were carried out using JASCO IR-5500 (Jasco Tokyo Japan) by high-performance reflection absorption spectroscopy (RAS). A reflection attachment was used at an

incident angle of 80° along with a wire grid polarizer. Electronic balance with measurement accuracy of 0.01mg (CP225D, Sartorius) was used to examine dissolving amount of aluminum in different supporting electrolytes and the polymeric nanofilm weight. Dissolving amount of aluminum (ppm) was calculated in the following method. The weight of dissolving aluminum before and after polymerization is divided by the weight of supporting electrolyte. X-ray photoelectron spectroscopy (XPS) was performed to investigate the elemental composition of aluminum surface with polymeric nanofilm. Spectra were obtained by using ULVAC PHI-5600 spectrometer equipped with monochrome Al $K\alpha$ radiation (1,486.6 eV). The pressure in preparation chamber was less than 10^{-7} Torr and less than 4×10^{-10} Torr in analysis chamber. Samples were examined over an area of $800 \times 2,000 \mu\text{m}$, and photoelectron spectra were recorded with a take-off angle of 45° . Nanofilm thickness was measured by using JASCO M-150i ellipsometer (Jasco Tokyo Japan) as the average value of three tests. The treated surfaces were observed by atomic force microscopy (AFM) (Nanoscope III Scanning Probe Microscope, Digital Instruments, Veeco Metrology Group) with contact mode to characterize surface morphology.

3. RESULTS AND DISCUSSION

3.1. Effect of supporting electrolyte on electrochemical polymerization

In order to find the optimal electrolyte for electrochemical polymerization of ATP on aluminum surface, the FT-IR spectra obtained after galvanostat polymerization were analyzed according to the previous result [15], which was in 0.1 M electrolyte solution containing 5 mM solute with a current density of $0.2\text{mA}/\text{cm}^2$ for 6 minutes at 25°C (Fig. 1). The results are totally different for the six electrolytes. As for NaNO_2 , the absorption bands centered at 1481 and 1560cm^{-1} are assigned to C=N and C-N groups of triazine ring [15]. Perfluorododecyl amino groups are confirmed by absorption peaks at 1226cm^{-1} , 1270cm^{-1} and 1155cm^{-1} due to C-F stretching vibrations of CF_3 groups and $>\text{CF}_2$ groups [16].

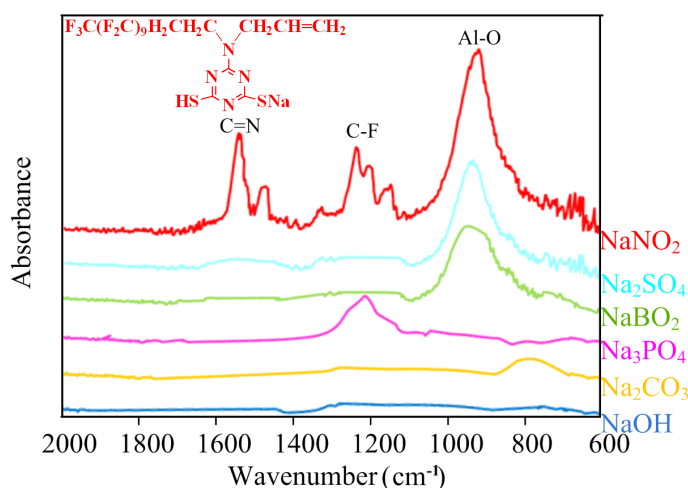


Figure 1. Structure of ATP (red color) and FT-IR spectra of electropolymerized aluminum plates using 0.1 M various electrolyte solutions containing 5 mM ATP with a current density of $0.2\text{mA}/\text{cm}^2$ for 6 minutes at 25°C

At the same time, the peak of alumina at 952cm^{-1} was also observed. It could be suggested that the electropolymerization of ATP and oxidative reaction of aluminum occurred simultaneously. However, typical absorption bands of triazine ring and CF groups could not be observed from FT-IR spectra with other supporting electrolytes.

Besides, there are even no absorption bands of Al_2O_3 while Na_3PO_4 (11.13), Na_2CO_3 (10.25) and NaOH (12.15) are used as electrolytes, which owes to the strong alkalinity reacting with Al_2O_3 and Al. Dissolving amount of aluminum before and after polymerization best illustrates this phenomenon (Tab. 1). In addition, the change of pH values before and after polymerization in NaBO_2 , Na_3PO_4 , Na_2CO_3 and NaOH electrolyte is slight, while pH of NaNO_2 and Na_2SO_4 electrolyte solutions varies drastically. Great variety of pH values reveal that electro-chemical reaction occurred in these electrolytes, which leads to the change of solutions. The above results indicate that NaNO_2 is the ideal supporting electrolyte for electrochemical polymerization of ATP on aluminum surface.

Table 1. The change of pH values and dissolving amount of aluminum in various electrolyte solutions

| Electrolyte | The change of pH values (before ~ after polymerization) | Dissolving amount of aluminum (ppm) |
|--------------------------|--|--|
| NaNO_2 | 7.17 ~ 9.28 | 1.9 |
| Na_2SO_4 | 6.28 ~ 7.46 | 1.5 |
| NaBO_2 | 9.61 ~ 9.74 | 3.1 |
| Na_3PO_4 | 11.13 ~ 11.38 | 8.6 |
| Na_2CO_3 | 10.25 ~ 10.31 | 2.7 |
| NaOH | 12.15 ~ 12.27 | 20.3 |

3.2. Effect of eletropolymerization current on polymeric nanofilm

Figure 2 demonstrates the relationship between potential and eletropolymerization time at different galvanostatic currents on aluminum surfaces. An acute increase of each curve in potential was observed due to the oxidation of aluminum and the formation of polymeric nanofilm [17]. For the five curves, the same terminal potential is reached since this the nanofilm has low conductivity and high resistance. However, the polymerization time increases as the current declines. In fact, we should avoid slow polymerization process because more oxides of aluminum will be produced with time prolonged at a low current. Therefore, currents at 0.3, 0.4 and $0.5\text{mA}/\text{cm}^2$ have similar electrochemical behaviors and the result preliminarily suggests that the optimal current is between 0.3 to $0.5\text{mA}/\text{cm}^2$.

Based on $E-t$ curve results, accurate atomic concentrations of PATP nanofilms prepared at 0.3, 0.4 and $0.5\text{mA}/\text{cm}^2$ were investigated to verify which current was the optimal. XPS data of PATP are shown in Figure 3. It can be seen that the atomic concentrations of C1s, S2p, N1s and F1s attain the maximum when the polymerization current is $0.4\text{mA}/\text{cm}^2$. Atomic concentrations show a diminution under higher currents. It is because that the insulating PATP generated on the aluminum surface at $0.4\text{mA}/\text{cm}^2$ blocks the charge transfer process.

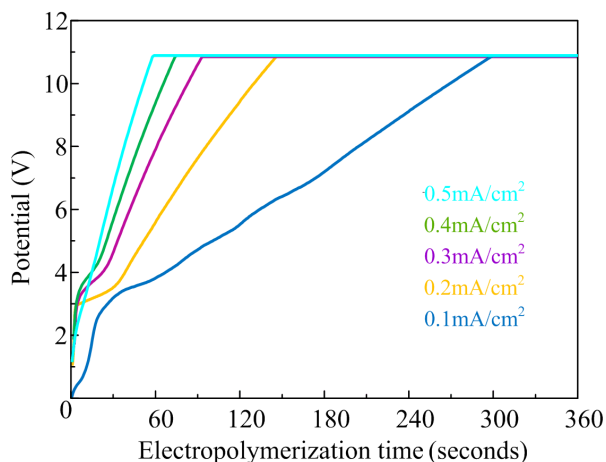


Figure 2. Relationship between potential and time (*E-t* curve) by galvanostatic on aluminum surfaces with polymerization currents ranging from 0.1 to 0.5 mA/cm² containing 5 mM ATP at 25 °C for 6 minutes in 0.1 M NaNO₂ electrolyte

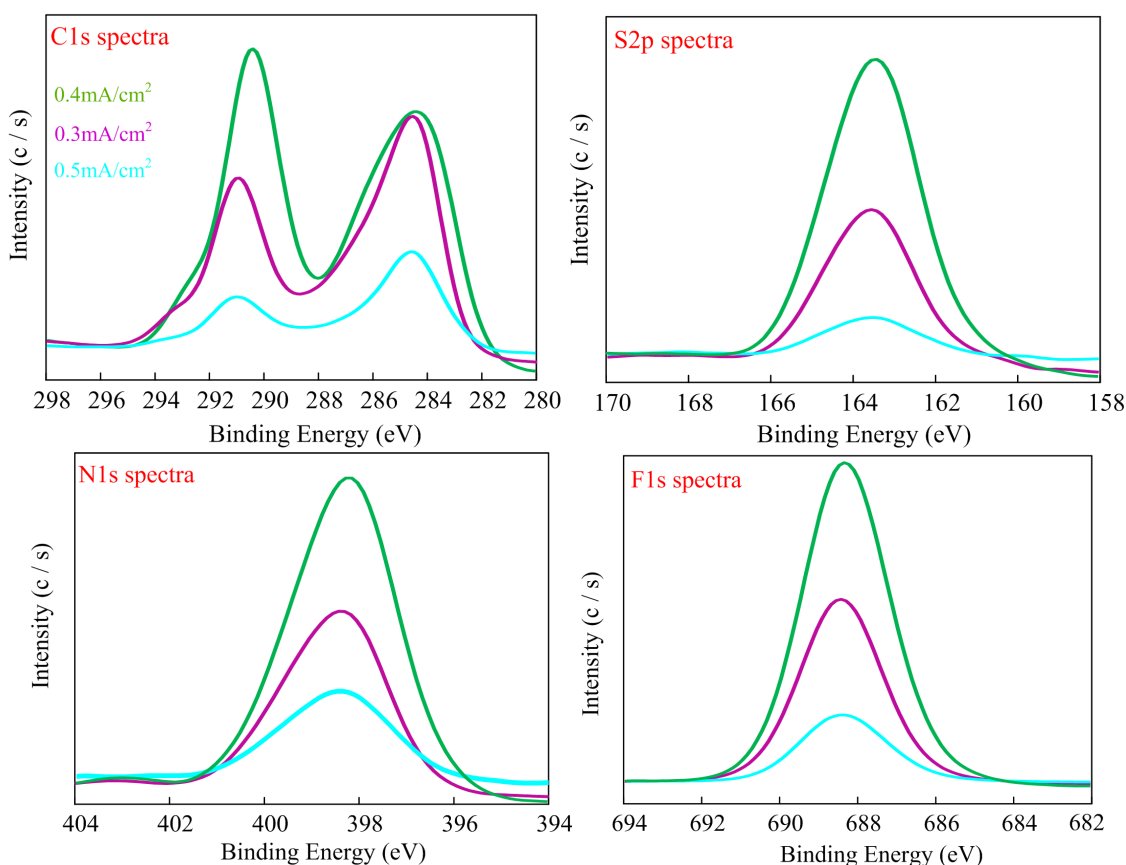


Figure 3. Effect of polymerization current on various elements in polymeric nanofilm by XPS analysis containing 5 mM ATP at 25 °C for 6 minutes in 0.1 M NaNO₂ electrolyte

Therefore, the PATP nanofilms did not form any longer even though the polymerization current increased. The polymeric nanofilm is destroyed to some extent due to the high current density

which forms an inferior quality, because the concentrations of the elements in PATP formed at 0.5 mA/cm^2 is even lower than 0.3 mA/cm^2 . This is the basic reason why we chose current range of 0.1 to 0.5 mA/cm^2 . In trial studies, bubbles generated from aluminum surface can be observed at higher currents over 0.5 mA/cm^2 . In brief, the XPS spectra results suggest that 0.4 mA/cm is the optimal current.

3.3. Effect of Electropolymerization Temperature on PATP Nanofilm

The relationship between electropolymerization potential and time at different temperatures on aluminum surfaces is exhibited in Figure 4. The same terminal potential is reached for the curves of temperatures by means of the oxidation of aluminum and the formation of polymeric nanofilm. With time prolonged, only potential curve at 35°C descends inordinately. It is presumed that the anion of triazinedithiol monosodium in the solution could diffuse to the aluminum surface very slowly, which influences the rate of the electropolymerization reaction. According to law of thermodynamics, we know that the diffusion rate of a monomer anion depends on temperature. Therefore, the stable potential achieves when the electropolymerization temperature is increased from 5 to 25°C . However, the oxidative reaction and stripping of aluminum could be accelerated at 35°C . The result preliminarily suggests temperatures at 5°C , 15°C and 25°C have similar results.

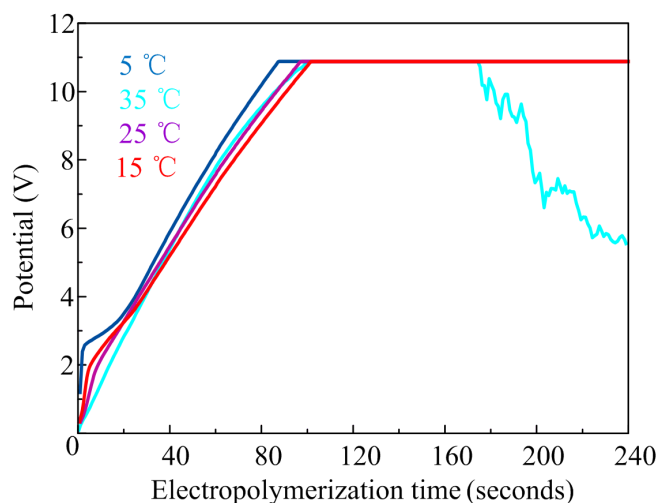


Figure 4. Relationship between polymerization time and potential ($E-t$ curve) on aluminum surfaces with current at 0.4 mA/cm^2 containing 5 mM ATP for 4 minutes at different temperatures in 0.1 M NaNO_2 electrolyte

The relation between film weight (Y) and the polymerization time (t) at different temperatures are investigated in Figure 5 based on above results. Nanofilm weight is determined from the difference in aluminum plate before and after polymerization. Y is found to increase suddenly within the first eight minutes and gradually thereafter [18]. The slope (5.6820) and correlation coefficient ($R^2=0.9836$) of the line at 15°C is the highest of all which indicate it is the ideal temperature. The peeling off of

PATP nanofilm happens and the nanofilm becomes loose due to the de-polymerization reaction with temperature increasing [19].

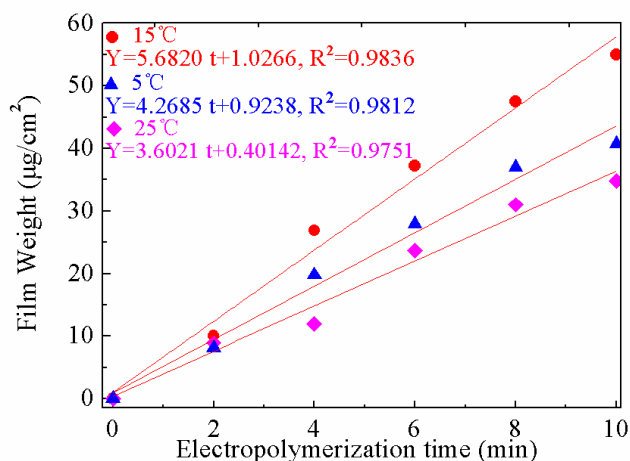


Figure 5. Relation between polymeric film weight and the polymerization time at 0.4mA/cm² containing 5 mM ATP for 10 minutes at different temperatures in 0.1 M NaNO₂ electrolyte

3.4. Effect of Electropolymerization Time on PATP Nanofilm

Figure 6 reports nanofilm thickness of PATP obtained by using different polymerization time. With electropolymerization times ranging from 3 to 8 min, the thickness value become larger. The thickness varies slightly when the polymerization time exceeds 8 minutes. It can be speculated that the PATP nanofilm obtained by galvanostatic polymerization for 8 min is more compact and insulated, which could depress the further formation of PATP nanofilm.

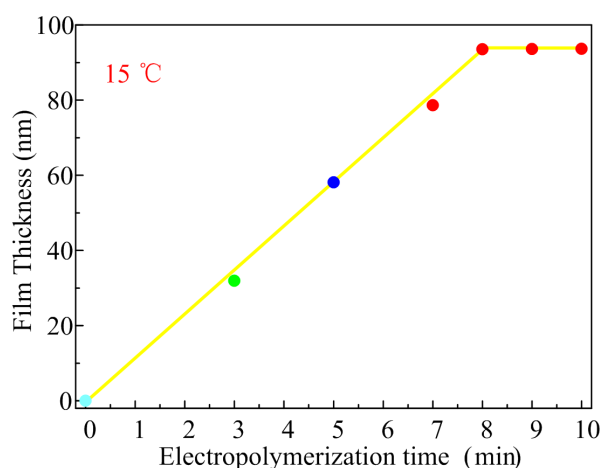


Figure 6. Relation between polymeric nanofilm thickness and the polymerization time at 0.4mA/cm² containing 5 mM ATP for 10 minutes at 15°C in 0.1 M NaNO₂ electrolyte

Moreover, the two dimensional morphologies of the aluminum surface were studied by AFM by different time in Figure 7. It can be observed that the aluminum surfaces are covered by PATP nanofilm when the polymerization time is increased [20]. The fringes of the aluminum reference surface disappear gradually due to the formation of the polymeric nanofilm from 5min to 8min. Also, the coverage of the polymeric nanofilm on the aluminum surface becomes larger. Island domain is uniformly distributed for eight minutes, and no obvious differences can be seen for the ninth minute. All of the results reveal that the optimal electrochemical polymerization temperature is 8 min.

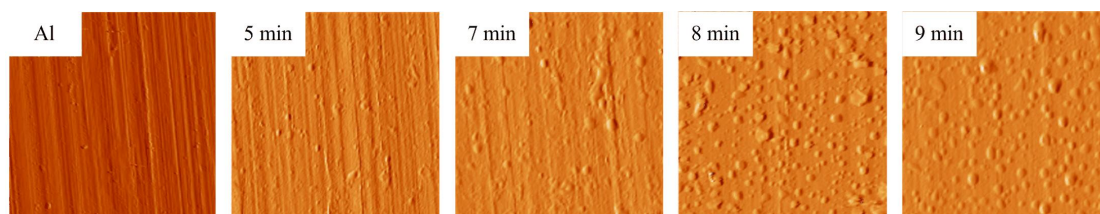


Figure 7. AFM images ($25 \times 25 \mu\text{m}$) of aluminum reference and PATP films covered on aluminum surfaces fabricated at different time

4. CONCLUSIONS

PATP functional nanofilm can be obtained successfully by using galvanostatic technique. The optimal process is that ATP (5mM) polymerizes with $0.4\text{mA}/\text{cm}^2$ for 8 minutes at 15°C in NaNO_2 electrolyte. Uniform and compact polymeric nanofilm of ATP could be obtained under these conditions. It is expected that this galvanostatic polymerization technique will be applied in preparation of lubricating, anti-tribological and hydrophobic surfaces on aluminum with superior quality using functional triazinedithiols.

ACKNOWLEDGMENTS

The authors gratefully acknowledge the Qinghai Technology Committee Industrial Public Relation Project of China (Grant 2012-G-204 and 2010-G-210) and the National Natural Science Foundation of China (Grant 21203152). We thank Dr. Milan Antonijevic and the reviewers for critical review of the manuscript.

References

1. K. Mori, Y. Okai, H. Horie, H. Yamada, *Corros. Sci.*, 32 (1991) 1237.
2. F. Wang, Y. Li, Y. Li, H. Zhang, *Int. J. Electrochem. Sci.*, 7 (2012) 3717.
3. Z. Kang, X. Lai, J. Sang, Y. Li, *Thin Solid Films*, 520 (2011) 800.
4. F. Wang, Y. Wang, Y. Li, Q. Wang, *Mater. Lett.*, 65 (2010) 621.
5. Z. Kang, Q. Ye, J. Sang, Y. Li, *J. Mater. Process. Tech.*, 209 (2009) 4543.
6. Z. Kang, W. Chen, Y. Long, K. Mori, Y. Li, *Mater. Sci. Forum*, 471 (2004) 871.
7. F. Wang, K. Mori, Y. Oishi, *Polym. J.*, 38 (2006) 484.
8. F. Wang, Y. Li, Q. Wang, Y. Wang, *Int. J. Electrochem. Sci.*, 6 (2011) 113.

9. G. Fang, Q. Liu, Z. Kang, F. Wang, *Tribol.*, 31 (2011) 534.
10. F. Wang, Y. Wang and Y. Li, *Int. J. Electrochem. Sci.*, 6 (2011) 793.
11. F. Wang, Y. Wang, Y. Li, Q. Wang, *Appl. Surf. Sci.* (2010) 2423.
12. F. Wang, Y. Wang, Y. Li, H. Zhang, J. Wang, *Int. J. Electrochem. Sci.*, 6 (2011) 1127.
13. K. Mori, H. Hirahara, Y. Oishi, N. Kumagai, *Mater. Sci. Forum*, 350 (2000) 223.
14. F. Wang, Y. Wang, Y. Li, *Int. J. Mol. Sci.*, 11 (2010) 4715.
15. K. Mori, Y. Sasaki, S. Sai, S. Kaneda, H. Hirahara, Y. Oishi, *Langmuir*, 11 (1995) 1431.
16. F. Wang, K. Mori, Z. Kang, Y. Oishi, *Heteroatom Chem.*, 18 (2007) 60.
17. Z. Kang, J. Sang, M. Shao, Y. Li, *J. Mater. Process. Tech.*, 209 (2009) 4590.
18. K. Mori, Z. X. Kang, J. Oravec and Y. Oishi. *Mater. Sci. Forum*, 419 (2003) 921.
19. J. Sang, Z. Kang and Y. Li. *T Nonfer Metal Soc*, 18 (2008) 374.
20. F. Wang, H. Luo, Q. Wang, J. Wang and J. Xu. *Molecules*, 14 (2009) 4737.